Journal Pre-proof

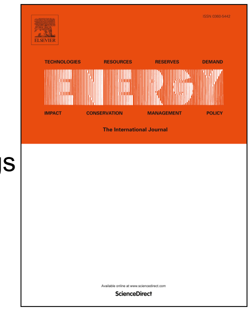

Performance and feasibility assessment of a hybrid cooling system for office buildings based on heat dissipation panels

Amaia Zuazua-Ros, Ramos Juan Carlos, César Martín-Gómez, Tomás Gómez-Acebo, Erell Evyatar

PII: S0360-5442(20)31082-3

DOI: https://doi.org/10.1016/j.energy.2020.117975

Reference: EGY 117975

To appear in: *Energy*

Received Date: 27 February 2020

Revised Date: 17 May 2020

Accepted Date: 25 May 2020

Please cite this article as: Zuazua-Ros A, Juan Carlos R, Martín-Gómez Cé, Gómez-Acebo Tomá, Evyatar E, Performance and feasibility assessment of a hybrid cooling system for office buildings based on heat dissipation panels, *Energy* (2020), doi: https://doi.org/10.1016/j.energy.2020.117975.

Credit Author Statement:

Amaia Zuazua-Ros: Conceptualization, methodology, writing - original draft; Juan Carlos Ramos: Software, validation; César Martín-Gómez: Conceptualization, investigation; Tomás Gómez-Acebo: Supervision; Evyatar Erell: Validation, Writing - reviewing and editing

1. Introduction

Energy use for space cooling is growing faster than for any other end use in buildings: it has more than tripled between 1990 and 2016, and is projected to increase as much as ten-fold in the coming years in some emerging economies, such as Indonesia and India [1]. Unlike other components of building energy demand, space cooling is not expected to decline by 2050 [2]. The main reasons for this increase are its rapid spread in developing countries, the effects of global warming and the overheating experienced in some highly insulated and airtight office buildings [3]. Hence, it is essential to develop more efficient types of cooling systems for various applications [4].

Passive cooling seeks to avoid the drawbacks inherent in all mechanical systems. Cooling strategies may be described according to how they manage excess heat: protection, modulation and dissipation [5]. All heat dissipation strategies require a thermal sink to absorb heat from the building, such as atmospheric air, the ground, water or the sky. In the latter case, outer space is treated as an infinite heat sink capable of absorbing energy emitted from man-made structures and transmitted through the atmosphere [6]. To cool a building, the heat dissipation element must either be cooler than the indoor temperature, or the cooling system should include a means of generating a flow of energy from a relatively low-temperature internal source to a warmer external element.

In night radiative cooling systems, both the sky and the ambient air are considered as the heat sinks. Unglazed solar collectors may be used for dissipation, and may be coupled to a storage tank [7]. Models of night radiative cooling systems have been based on existing methods used to describe flat plate solar collectors [8] and several variations and alternatives for water based night radiative systems have been explored [9]. The performance of thermal collectors for night radiative cooling has been studied, such as PVT-water collectors [10] or three different types of radiative-convective panels by Tevar et al. [11] and Erell and Etzion [8]. This last study also analyzed the importance of convective dissipation. The inclusion of phase-change materials has also been analyzed in [12], where the storage tank included micro-encapsulated phase change material slurry. This solution appears to be a good medium for the combined application of passive cooling technology and nocturnal radiation in an air conditioning system due to its relatively high working temperature. Recently, the performance of conventional PV panels with nocturnal radiative cooling has also been studied to generate electricity and obtain cooling energy [13]. The same research team has gone a step further proposing a strategy for building integrated PV and daytime radiative cooling [14].

While nocturnal radiative cooling systems are relatively well documented [15–19], daytime radiative cooling is still an emerging field [9]. Recent advances have demonstrated highly selective surfaces capable of producing sub-ambient temperatures during daytime and under direct solar radiation, in certain conditions [20,21]. Such systems are technological marvels, but suffer from three inherent limitations:

a. If the radiator surface temperature is not substantially lower than the desired *indoor* air temperature, the cooling potential of the surface cannot be realized, irrespective of its temperature relative to *outdoor* air (although it may still reduce unwanted heat gains, much as thermal insulation does). For example, if the desired internal air temperature is 24 degrees, the radiator should be cooler than 22 degrees, and preferably much cooler still.

b. The high albedo required by thin film coatings for daytime cooling is difficult to maintain in a real urban environment due to external factors such as deposition of dust, dew and air pollution. This is an inherent drawback of all highly selective surfaces, which require constant maintenance to preserve their unique optical qualities.

c. Sub-ambient air temperatures are especially difficult to achieve in windy conditions, irrespective of the radiant properties of the surface. Use of windscreens, as suggested by several studies, is ineffective because the surface of the windscreen becomes itself soiled over time, and masks the primary radiator surface.

Thus far, none of the prototypes that rely on such surfaces has been demonstrated in a real building-integrated scenario over an extended period of time. The conventional approach to air conditioning has therefore relied on mechanical systems, in which excess heat is pumped from the building interior to an exterior heat exchanger, typically a cooling tower. Many modern office buildings use cooling towers to dissipate to the atmosphere the waste heat accumulated in a cooling fluid. Open circuit cooling towers cool the water coming from the condensers by evaporation, distributing the water to be cooled by spray nozzles in the tower. Thus, the water in contact with the atmospheric air cools down. A portion of water absorbs heat and changes from liquid to vapor state and is absorbed in the air stream [22]. The main drawbacks of this equipment are the high use of water, risk of legionella disease, high maintenance requirements, high operational cost and the noise and vibrations caused by the fans [23]. Water quality and use in particular are a topic of concern in the interaction of cooling towers with the environment [24]. Air condensation systems, dry coolers in particular, are an alternative to cooling towers, given that they do not consume water and the risk of legionella is non-existent. However, they too have disadvantages, such as a lower efficiency, higher electricity consumption (due to the fans), greater space requirements and noisy equipment [25].

This paper presents an alternative to both cooling towers and passive radiant cooling systems: a hybrid radiative cooling system that aims to reduce or eliminate the problems associated with cooling towers by using dry heat dissipation panels coupled to a cooling system with a pumped heat transfer fluid. Unlike completely passive systems, which rely on a natural driving force for fluid circulation [26], this hybrid system incorporates mechanical elements and requires an external source of electrical energy to operate. The heat dissipation panels are not connected directly to a storage tank and then to the building. Instead, they are connected to a chiller's condenser, replacing a cooling tower. Thus, the working temperature of the panels loop included in the hybrid system presented here is higher than the temperature of previous passive radiative cooling systems since the condenser of chillers work at higher temperatures, which makes its daytime operation viable without the use of high-albedo thin film coatings. The higher temperature improves heat dissipation ratios compared to passive radiative cooling. The present paper takes this approach one step further, considering not just the cooling panel in isolation but also the performance of the system as a whole, as installed in a building.

The paper is structured as follows: (1) description of several hybrid system configurations; (2) performance of the modelled hybrid system scenarios, relative to each other and to a conventional system; and (3) evaluation of the overall feasibility of the proposed system and further optimization for future implementation possibilities.

2. Methodology

In order to analyze the system performance and feasibility of the hybrid system, a case study was performed using a real office as a reference. Because radiant cooling systems have hitherto been required to cool the interior directly, they have been located on roofs, to take advantage low effective sky temperature. This has limited their application to low-rise buildings, especially in very dry climates. Because the hybrid system proposed here incorporates heat dissipation panels in the form of vertical fins attached to building facades, the configuration allows implementation in multi-story buildings [27,28].

2.1 Cooling panels

Figure 1 provides a schematic description of the cooling panels used in the study. The present study incorporates an analytical model developed for this application previously and validated with experimental data [23,29]. The cooling capacity for each operation scenario (fluid flow rate and temperature at the inlet) depends directly on the dry bulb temperature of the ambient air and on the incident solar radiation. Further details on the model are provided in the Supplementary Information available in the online version.

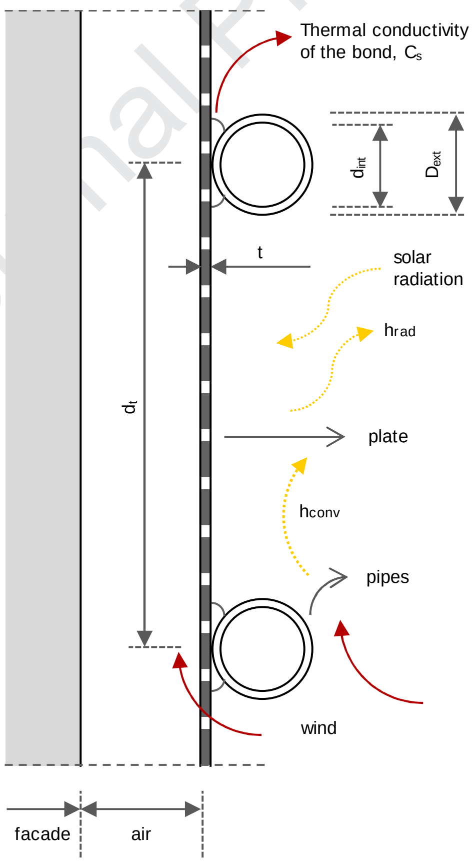

Figure 1. Schematic section of the cooling panel and heat transfer factors.

2.2 Description of the whole-building hybrid cooling system

The hybrid cooling system is based on the use of cooling panels to dissipate heat in support of a water-to-water chiller or a heat pump in cooling mode, to reduce the use and operation time of cooling towers. An initial configuration of a conventional system is used as a reference and as a basis to create the hybrid system. The initial system is shown in the left side of Figure 2, labelled as system C1.

The chiller is the core of the system, dividing the heat absorption side and the heat rejection side. There are two loops on the heat absorption side. The circuit formed by the building and the buffer tank is referred as the building loop: it absorbs the initial peak demands of the building. The loop formed by the buffer tank and the chiller's evaporator is the chilled loop. In this configuration, heat rejection is made through an open-circuit cooling tower. The loop formed by the cooling tower and the chiller's condenser is referred to as the 'cooled loop'. Each loop requires its own pump. Two possible hybrid cooling systems (labelled C2 and C3) are then analyzed, which are variants of the base configuration (C1): the arrangement in the heat absorption side is unchanged and the heat rejection side of the system is modified.

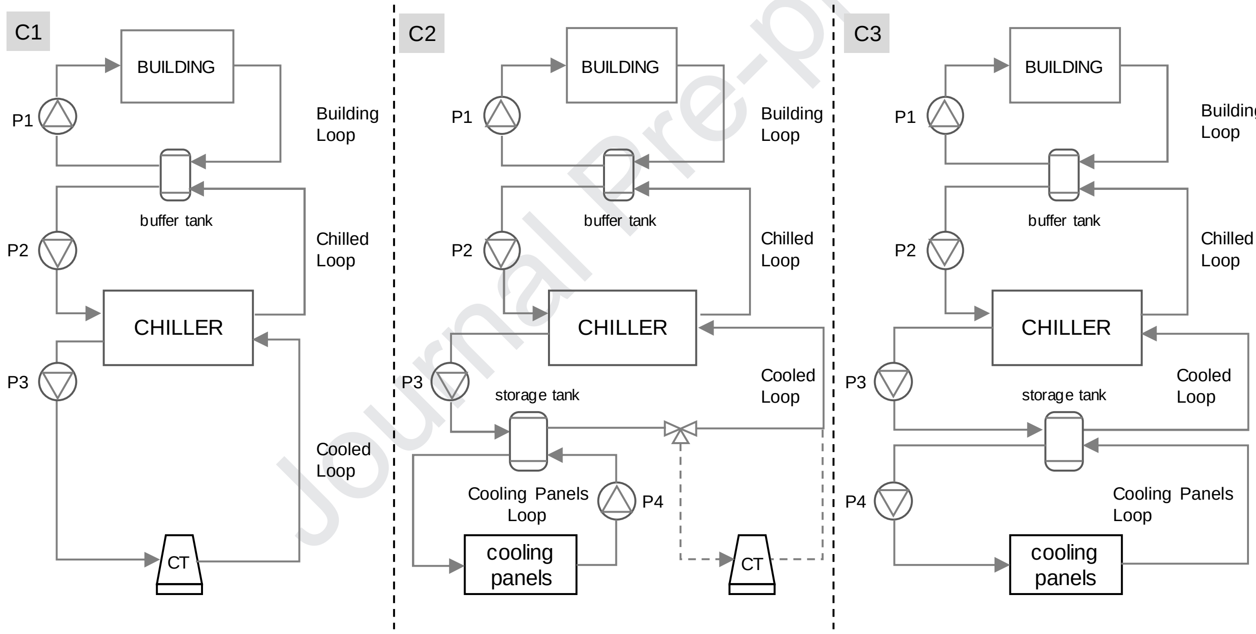

Figure 2. Three configurations simulated. C1 (left) corresponds to a conventional system, while C2 and C3 represent two possible designs of the hybrid cooling system.

Configuration C2 (middle panel in Figure 2) is a hybrid cooling system with cooling panels coupled in series to the previous configuration. The capacities of the equipment are summarized in Table 4. The heat rejected from the condenser is first dissipated by the cooling panels through the storage tank. When this is not enough to achieve the designed return temperature to the chiller, the by-pass to the cooling tower operates to dissipate the heat. The cooling panels and the storage tank form an additional loop, referred to in the figure as the 'cooling panels loop'. This configuration requires an additional pump (P4).

The third configuration (C3 in Figure 2) shows a hybrid cooling system with cooling panels only, completely replacing the cooling tower. The aim is to reject the heat exclusively by the cooling panels. The cooled water loop and the cooling panels loop are needed due to the installation of the storage tank.

The parameters considered are the energy consumption of the chiller, the pumps and the cooling tower fan. In addition, since the considered system is an open circuit cooling tower, water consumption has a significant role. Given that the cooling panel loop always operates with a storage tank, the hybrid systems will always need an additional hydraulic pump compared to the reference system.

The chiller is the element that generates cooling in the system. When calculating and choosing a chiller, the condenser inlet temperature ($T_{cond,in}$) is the key parameter to evaluate performance. Figure 3 shows the performance graphs provided by the manufacturer [30]. As shown in the left axis of the graph with the grey lines, increasing the inlet temperature will lower the system COP. The figure also reflects the relationship between the cooling capacity and the fluid flow rates of the evaporator and condenser (red lines and right axis): to provide a greater cooling capacity higher fluid flow rates are needed in each loop. The panels' surface area thus limits the cooling capacity of the system.

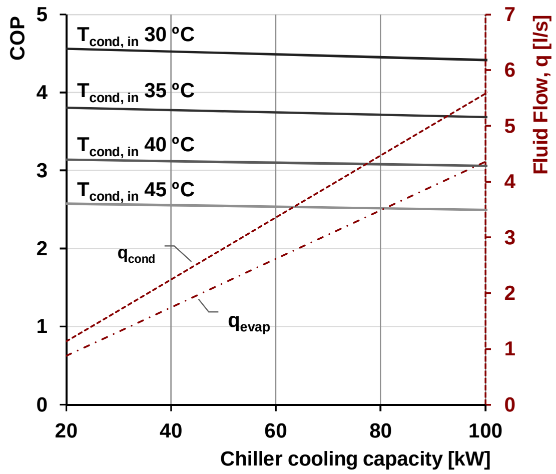

Figure 3. Chiller performance data and fluid flow rate conditions in relation to the cooling capacity for a cooled water inlet temperature of 10 °C.

Since one of the factors affecting the energy consumption of the chiller is the condenser inlet temperature, the storage tank must be installed in the cooling panels loop to maintain a steady temperature, as far as possible. Without the storage tank, heat dissipation is highly sensitive to the cooling panels' performance in adverse external conditions.

Therefore, three configurations are simulated; two configurations including the hybrid cooling system (C2 and C3) are compared to a base system (C1), which is a conventional water-to-water system with a cooling tower. The data used in the simulations correspond to a real installed system which is described in the case study that is presented in Section 3.

2.3 Description of the office building

The reference building used as case study is an existing 3-story office building. The technical data from the building services related to the cooling system design for this building were used as a baseline for the simulation of the conventional system and then adapted to simulate the new hybrid system. Each story has a floor area of 875 m^2, for a total area of 2,625 m^2 (Figure 4).

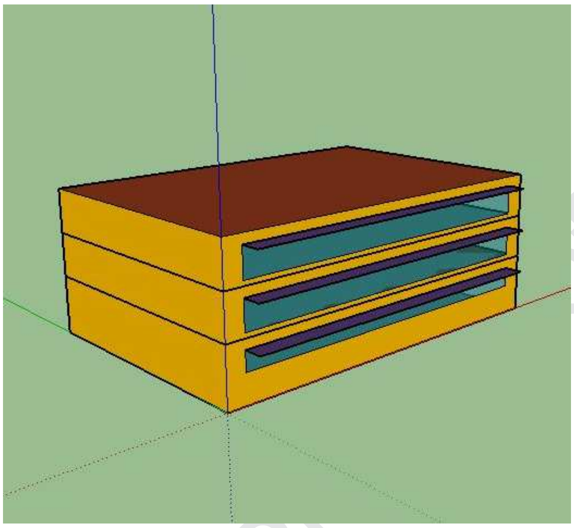

Figure 4. Office building model.

2.3.1 Office building construction elements

Table 1 summarizes the U values of the envelope elements. The right column represents the building standards of the CTE (Spanish Building Code) for this typology of building and for this location. All elements of the building meet the standards [31].

Table 1. Construction elements of the office building.

Element	U-value (building) [W/m^{2}K]	U-value (CTE) [W/m^{2}K]
Ground	0.33	0.5
Walls	0.25	0.73
Roof	0.33	0.41
Windows	1.43 (glazing) 20% frame/window	2.2 – 3.9 *

* The U value of the windows set by the code depends on the orientation of the façade.

The window and wall ratio have been taken from the original building. Window openings facing south correspond to 63% of the façade (99 m^2 per floor) and the openings facing north are 19% of the façade. There are no windows in the east and west orientations.

The occupancy of the building follows a working day schedule from Monday to Friday from 7 am to 7 pm. Table 2 summarizes the indoor environment and other internal gains, including lighting and equipment heat gains. The heat gains parameters correspond to the office areas. Given that the ground floor is mainly a storage room, the heat gains shown in the table only affect to a quarter of the area, except the lighting, which is maintained in the whole floor.

Table 2. The parameters of the indoor environment of the building.

Infiltration	0.5 ach
Cooling setpoint temperature	24ºC
Heat gains	
Occupancy	10 m^2/person
(Seated, light work typing)	75 W latent, 75 W sensible (ISO 7730)
Equipment - Computers	140 W/person
Lighting	10 W/m^2

The minimum ventilation rate for this building, according to the Spanish regulation for thermal installations in buildings (RITE) is 2.5 air changes per hour. However, the original building has a complex earth-to-air heat exchanger combined with a natural ventilation system that requires much higher ventilation rates. Since ventilation is not the focus of the study, a simplified system is modelled, in which the air change rate is fixed at 5 ach at daytime and 2 ach during night. During daytime, air is supplied at the outdoor ambient temperature, if this is between 18 and 23ºC; otherwise, the ventilation air is supplied at 20ºC. At night, the building may benefit from free cooling if the indoor temperature is higher than 23ºC. Otherwise, there will be no ventilation. The cooling load obtained in the simulation (see section 4.1.2) is thus similar to the system installed in the building. The cooling system actually installed in the building is a chilled ceiling, which is simulated taking the default characteristics specified in TRNsys.

2.3.2 Climatic conditions and cooling loads

The simulation is performed for Bilbao (northern Spain, 43°18'4" N, 2°54'38" W), which is the closest location to the actual experimental site (San Sebastian, 43°18'15" N, 2°0'35" W). The annual temperature and humidity of Bilbao is shown in Figure 5. Since it is very close to the coast, the relative humidity is between 57 and 96% during the whole year.

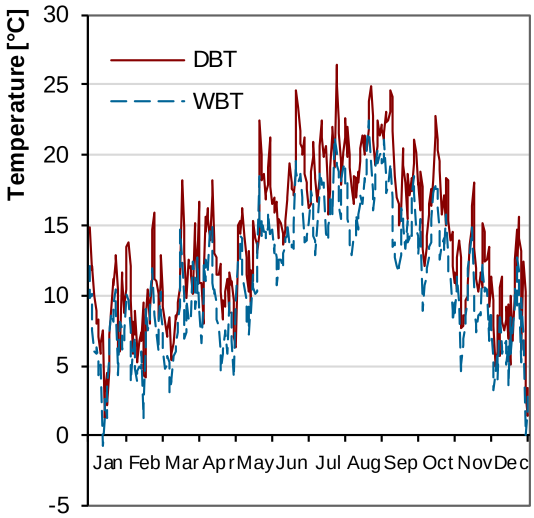

Figure 5. Dry bulb and wet bulb temperatures of Bilbao (mean daily values from TMY)**.**

The hourly dynamic loads of the building are the basis for the dimensioning of the cooling system. In Figure 6 the representative results obtained from an initial simulation of the cooling demand for the whole year is shown.

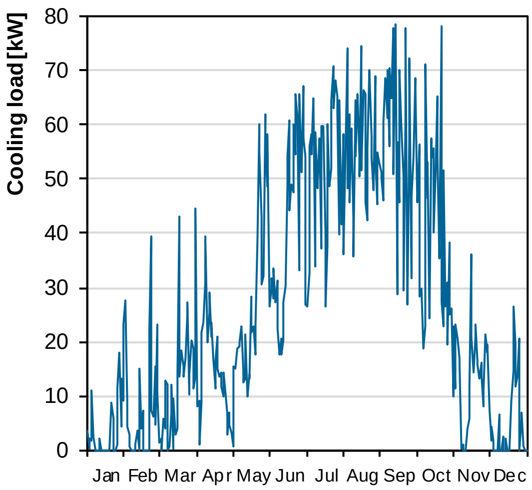

Figure 6. Annual distribution of the daily maximum cooling load of the building.

From the building performance analysis, it can be concluded that there is cooling demand almost every day of the year, due to the internal heat gains of the office (88% of the days). The total cooling demand is 65.9 MWh per year (approximately 47 kWh/m^2) with a peak demand of 78.5 kW. 89% of the total demand occurs between May and October.

2.4 System simulation parameters

The hybrid cooling system simulation was performed with TRNsys 17, which is a component-based software to simulate extensive alternatives of dynamic systems in buildings [32]. TRNsys uses subroutines (named *types*) which afterwards set up the systems to be simulated. The following subsections present the general parameters used in TRNsys and other considerations for each simulated configuration.

2.4.1 Cooling panel component

A new *type* was defined and compiled for TRNsys using the model provided in the SI in order to define the component that resembles the panel previously tested. Windows Visual Studio 2013 with Intel Parallel Studio XE was used for the Fortran coding and for the compilation.

Table 3. Inputs and parameters defined for the cooling panel subroutine in TRNsys.

Inputs			**Parameters**		
Inlet temperature	T_{in}	ºC	Panel area	A_p	m^2
Ambient temperature	T_{amb}	ºC	Fluid specific heat	c_p	kJ/kg K
Fluid flow rate	q	kg/h	Solar absorptivity	α_s	-
Solar radiation on surface	$\dot{S}$	W/m^2	Emissivity	ε	-
Wind speed	v	m/s	Efficiency factor	F’	-

The parameters and inlet conditions for the *type* of the panel are summarized in Table 3. While the inputs values are variable with regard to time, the parameters are constant values.

The cooling panels loop in configurations C2 and C3 comprised 168 panels (a total of 403.2 m^2 of cooling panel surface), placed according to the actual north façade of the building. The tank dimension was determined according to the Spanish Building Code (CTE). In the code, the recommendations for solar collector systems tanks vary between 50 and 180 liters per m^2 of panels. Using the lowest value, taking as a reference the storage used in [33], a storage tank of 20.1 m^3 is modelled and simulated.

2.4.2 Hybrid system

The remaining *types* used in the simulations are default components provided by TRNsys or by the Tess Library catalog. Figure 7 shows a screenshot of the system arrangement in configuration C2. The installed chiller is a vapor compression water-to-water chiller that corresponds to TRNsys *type* 666.

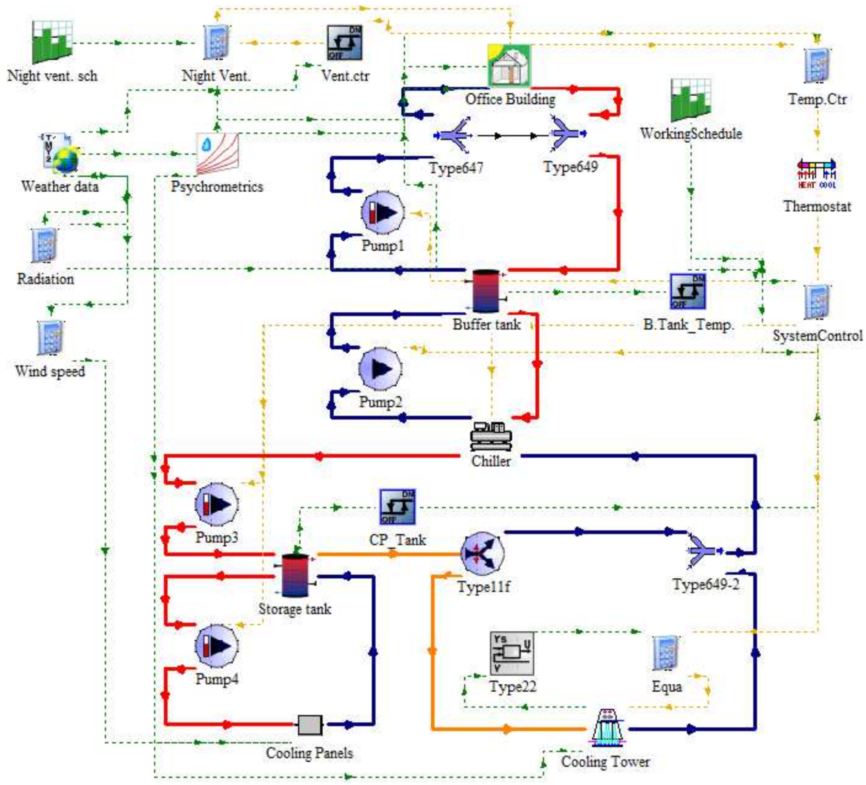

Figure 7. TRNsys interface screenshot for C2 configuration.

Each of the four to five hydraulic loops that are labeled, depending on the system configuration, have a hydraulic pump. The pump of the building loop, P1, is a variable speed pump (*type* 110) and the pumps P2, P3 and P4 are constant speed pumps (*type* 3). The electricity consumption of the pumps (P1, P2, P3 and if necessary, P4), as well as the energy consumption of the tower's fan, are considered in the yearly total consumption analysis.

A preliminary simulation must be done to study the cooling power needed. The component specified as a water-to-water chiller requires definition of the setpoint temperature of the cooled water, the rated capacity and the COP, which depend on the inlet temperature of the condenser. In other words, the behaviour of the cooling panels and the storage capacity will affect the chiller's performance. This performance is defined in the TRNsys subroutine for *type 666.* No modifications were made to this calculation method for the simulations presented in this study. The parameters used for each *type* of the simulation are summarized in Table 4.

Table 4. Main parameters used for simulation configurations

Pumps and Fan			**$C1_{T30}$**	**$C1_{T35}$**	**C2**	**C3**
Pump 1	Power	kW	1	1	1	1
	Fluid flow rate	kg/s	5.5	5.5	5.5	5.5
Pump 2	Power	kW	0.8	0.8	0.8	0.8
	Fluid flow rate	kg/s	3.71	3.5	3.71	3.5
Pump 3	Power	kW	1	1	1	0.6
	Fluid flow rate	kg/s	4.5	4.38	4.5	4.38
Pump 4	Power	kW	-	-	1	1
	Fluid flow rate	kg/s	-	-	4.2	4.2
CT fan	Power	kW	1.1	1.1	0.75	-
	Air flow rate	m^3/s	3.94	3.84	3.94	-
Chiller	$Capacity_{rated}$	kW	78.0	73	78.0	73
	COP_{rated}	-	4.56	3.78	4.56	3.78
	Cooled T_{sp}	°C	10	10	10	10

Two design conditions have been considered for configuration C1. The difference between configurations $C1_{T30}$ and $C1_{T35}$ is due to the condenser inlet temperature condition. The first case, set at 30ºC, corresponds to a chiller capacity of 78 kW with a COP of 4.56. When the inlet temperature of the condenser increases to 35ºC, both the capacity and the COP decrease to 73 kW and 3.78, respectively. This decrease of capacity also affects slightly the fluid flow rates of those pumps connected to the chiller loops. The consideration of these two configurations is due to the chiller performance conditions of C2 and C3. In C2, the cooling tower ensures a constant condenser inlet temperature of 30ºC. However, in C3 the average water temperature outlet from the storage tank to the chiller is 34ºC for the climate of Bilbao. The rated capacity of the chiller is then lower than the cases that include cooling towers, and consequently, the COP is lower. Therefore, $C1_{T30}$ can be compared to C2 and $C1_{T35}$ to C3. As defined in the table, the fluid flow rates of the loops also vary. All data are taken from the manufacturer (Figure 3). The pumps power is maintained almost equal at each scenario except for P3 in C3, where the pressure drop is reduced by the proximity of the chiller and water storage tank.

For configurations that include a cooling tower, an open circuit cooling tower *type* has been used (*type* 51). The fan speed of the tower is controlled with an iterative feedback controller (*type* 22) in order to ensure the required constant temperature. In regard to the cell flow rate of the tower, a relation of L/G of 1 is considered [34], where (L (liquid) is the mass water rate entering the tower (in kg/s) and G (gas) is the air flow rate through the tower (in kg/s, converted to m^3/s with an air density of 1.14 kg/m^3).

The water consumption of the cooling tower is one of the parameters analyzed below. Cooling tower water consumption has three components: Firstly the evaporated water, which is around 1% of the circulated water. Then, the blowdown water, which corresponds to the water that must be bled from the recirculated water to prevent the high concentrations of soluble minerals [24]. Finally, spray drift, the small water droplets that are carried to the atmosphere. The drift, although small in quantity (0.005%)

[24], is the main means of propagation of legionella. Total water consumption is the sum of the evaporated water and blowdown water.

In TRNsys *type* 51, the level of the sump is assumed to be constant and the water consumption corresponds only to the evaporated water. Hence, an approximation of blowdown water must be made. The blowdown water is defined by the Cycles of Concentration (COC) of the system, which is the correlation between the system feed water and the blowdown water. This correlation depends mainly on the quality and characteristics of the local grid water, and its value may vary between 3 and 6 [35]. From a water efficiency standpoint, the higher the COC the higher the efficiency, since water consumption is lower. In this case, a COC of 5 is considered [36]. The final water consumption is given by Equation 1, based on a relation between COC, evaporated water and make-up water [37].

$$blowdown = \frac{evaporation}{COC-1} \qquad (1)$$

2.4.3 *Weather file considerations*

The weather data file used for the simulations is a TMY2 file from Bilbao airport (Spain), which is the closest location to the experimental site. In this file, the wind velocity is considerably higher than the average wind velocities recorded in the experimental site, given that the weather file is from an airport. Since wind velocity is a significant parameter in the model, a wind transformation equation has been applied to the simulation in order to adapt the wind velocity to an urban environment. The transformation requires only the displacement height and roughness length of both sites (A corresponds to the airport and B, to the location of the building).

Then, to calculate the wind speed $U(Z_B)$ at height Z_B (10 meters) in terrain B from a wind speed measurement $U(Z_A)$ taken at height Z_B (10 meters) in terrain A, equation (2) is used [38]:

$$\overline{U}(z_B) = \left(\frac{z_{0B}}{z_{0A}}\right)^{0.09} \frac{\ln\left(\frac{z_B - d_B}{z_{0B}}\right)}{\ln\left(\frac{z_A - d_A}{z_{0A}}\right)} \overline{U}(z_A) \qquad (2)$$

At the test site (location B), the zero-plane displacement (d) was set at 5 meters and the roughness length at 1 meter. The roughness length of the airport is 0.01 meters and the zero-plane displacement (d) is 0.

Regarding the solar radiation, the global radiation data from both TMY2 and the Spanish Building Code CTE matches, but there was a considerable difference between them in values of diffuse and beam radiation. For example: during the month of June the diffuse radiation is on average 1.35 times higher in the TMY2 file than in the building code, whereas the beam radiation is 0.76 times lower than in the code. Simulation results using the Spanish code data showed a better fit with experimental data, so a factor of 0.7 was applied to the diffuse radiation and 1.25 to the beam radiation, based on the average differences of the whole year.

2.4.4 *Control system*

The control system used in the simulation is shown schematically in Figure 8. It starts with a working hours schedule for the cooling system, set from 6 am to 19 pm. With the first stage set point temperature set at 22ºC, the building loop starts operating with the buffer tank. Then, if the second stage temperature is achieved (23ºC), the chiller starts working together with the chilled loop and the cooled loop pumps. The cooling panels loop operates independently. The set point of the storage tank is defined below 30ºC, which is the initially designed return temperature for the condenser of the chiller. It must be noted that the startup of the system causes a sudden increase of the temperature of the storage tank. To address this, the set point temperature of the panels loop tank is set at 26ºC.

All configurations have been simulated with a 0.1 hour time step for the whole year.

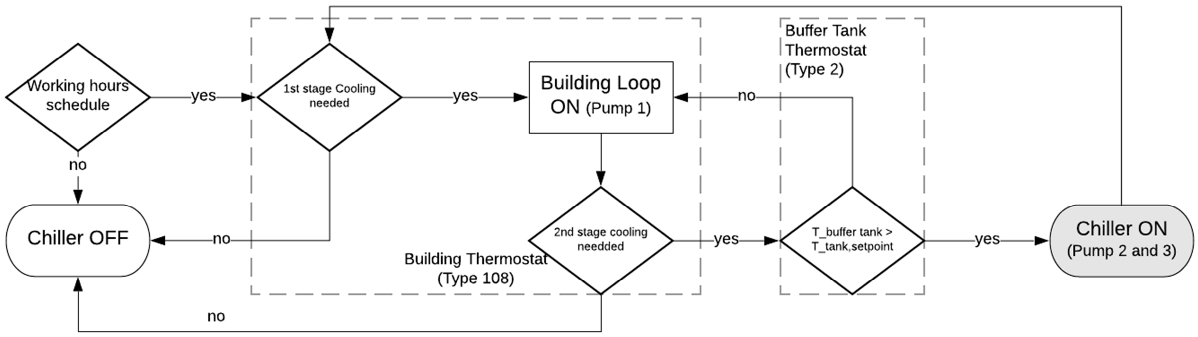

Figure 8. Control strategy for the building's cooling system.

3. Analysis of the results

The potential of cooling panels to replace a cooling tower is analyzed. Then, the cooling panels' performance in each configuration is evaluated. Finally, the complete system performance is studied. It must first be emphasized that the set point temperature of the building defined in the simulations is met in every configuration studied.

3.1 Cooling panels performance

The heat dissipation of the panels ($\dot{Q}$/A) and the inlet and outlet temperatures are investigated to study the behavior of the cooling panels under different conditions. Figure 9 shows the annual results for inlet and outlet temperatures and heat dissipation of the panels in configuration C2, where a cooling tower is also working. The average inlet temperature of the panels is 32.6ºC, with a standard deviation of 0.8ºC, while the outlet temperature is 30.2 and 1.5ºC of standard deviation. From these values, the mean heat dissipation ratio obtained is 104.9 ± 31.7 W/m^2 and in this scenario, a maximum cooling output of 234.5 W/m^2 has been achieved.

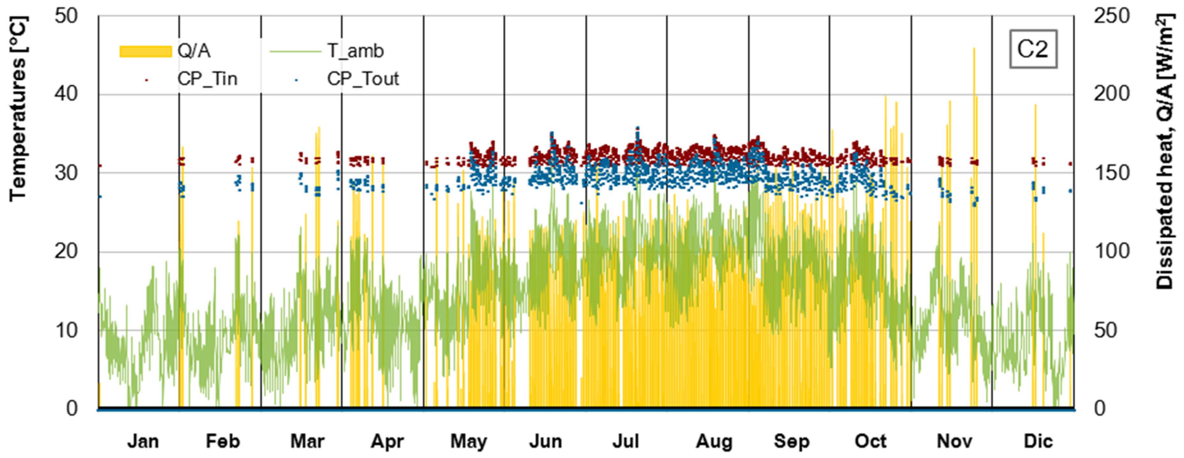

Figure 9. Configuration C2: annual cooling panel performance.

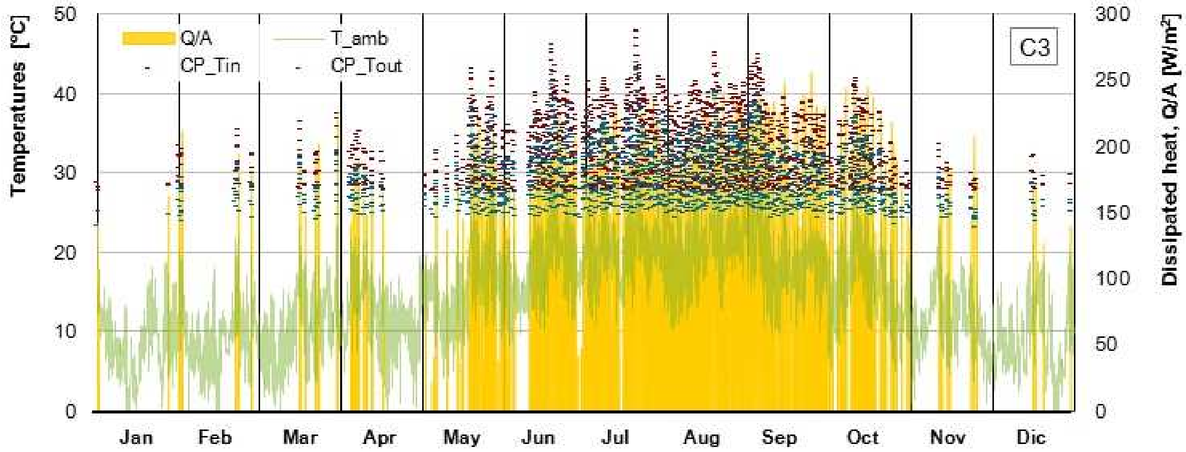

Figure 10. Configuration C3: annual cooling panel performance.

The values obtained with configuration C3, however, vary noticeably, as shown in Figure 10. In this case, the mean inlet temperature is 34.1°C with a standard deviation of 4.0ºC and the outlet 30.7°C with a standard deviation of 3.5ºC. These working temperatures are more unstable, as indicated by the increase of the standard deviation. Accordingly, the temperature difference between the outlet and the inlet also increases, giving an average heat dissipation ratio of 147.0 W/m^2 with a maximum of 271.2 W/m^2.

The inlet temperature difference between the two configurations is given because the cooling tower in C2 always lowers the temperature of the fluid entering the condenser of the chiller to the desired working temperature, in this case 30ºC. In this case, the condenser of the chiller is always working at constant temperature. However, when the cooling tower is eliminated in configuration C3, the cooling panels are not always capable of maintaining the storage tank temperature at a constant value of 30ºC, as is the case with the cooling tower. Consequently, the working temperature of the condenser in the chiller increases during warm days where the cooling capacity of the panels is lower.

The performance of the two configurations of the hybrid cooling system is now illustrated for two entire days: The warmest day of the year, 21st of July, and a mid-April day are represented in Figure 11 for C2 and Figure 12 for C3.

In Configuration C2, the cooling tower outlet temperature is always 30ºC, for both days, as defined. However, the cooling panels' outlet temperature varies in response to changes in ambient air temperature. Since the condenser inlet temperature is constant, the condenser outlet temperature can be considered constant, except for short periods following the daily starting up some brief starts and stops of the chiller during the day.

In July, as the ambient temperature increases, the panels' inlet temperature also increases, reflecting increased building cooling loads, and so does the average tank temperature, due to the inability of the panels to lower the fluid temperature in the tank to the desired level. The direct sunlight in the last hours of the day plays a relevant role, since there is no heat dissipation from 6 pm until the chiller is off (the dark grey area in the figures corresponds to the chiller working time). Conversely, in April the heat dissipation ratios remain between 125 and 145 W/m^2 during the entire day.

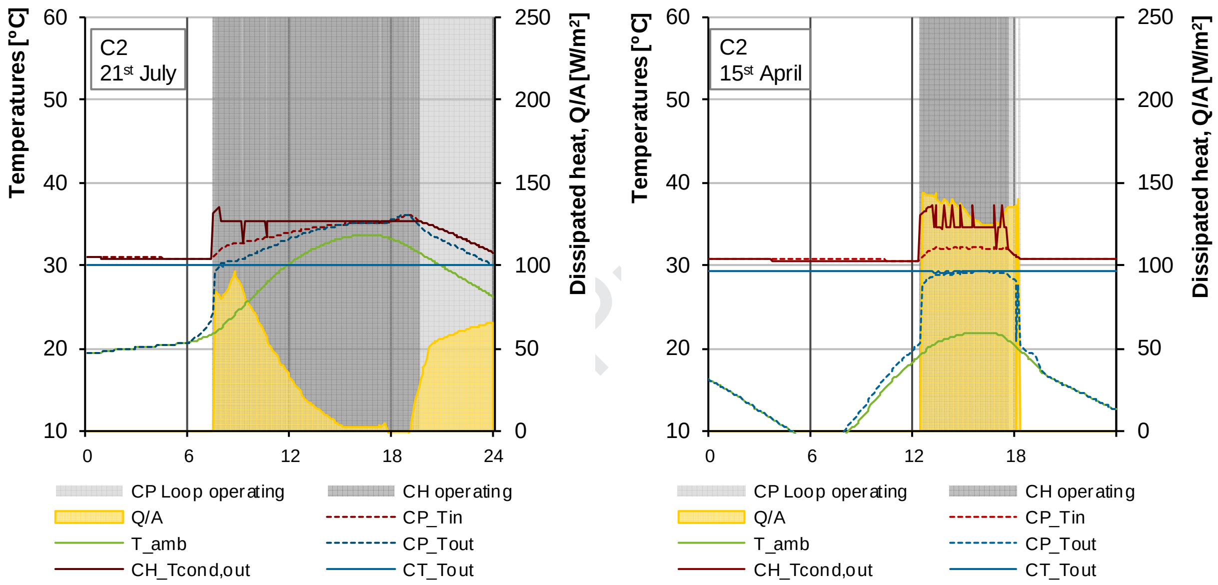

Figure 11. Cooling panels' performance during two representative days in Configuration 2.

In C3 (Figure 12), there is no cooling tower, so the heat dissipation can only be met by the cooling panels. In both representative days the panels' outlet temperature increases gradually, as does the condenser outlet temperature. In the most unfavorable day of the year, the 21st of July, the working temperatures of the cooling panels increase gradually. The condenser outlet temperature reaches the annual maximum of 53°C, while the outlet temperature of the panels reaches 43ºC. When the chiller stops working the temperatures decrease and the cooling panel loop continues operating (light grey area). The heat dissipation ratios are always higher than 50 W/m^2, exceeding 200 W/m^2 in the late afternoon.

The same working profile is observed in April, but the temperature profile is lower. The condenser outlet temperature reaches 40ºC at the end of the day. Consequently, the cooling panels' outlet temperature, which starts at 26ºC, increases to 32ºC. When the chiller stops working, the cooling panels loop continues operating until the temperature of the tank reaches 26ºC. The heat dissipation ratios are between 100 and 200 W/m^2.

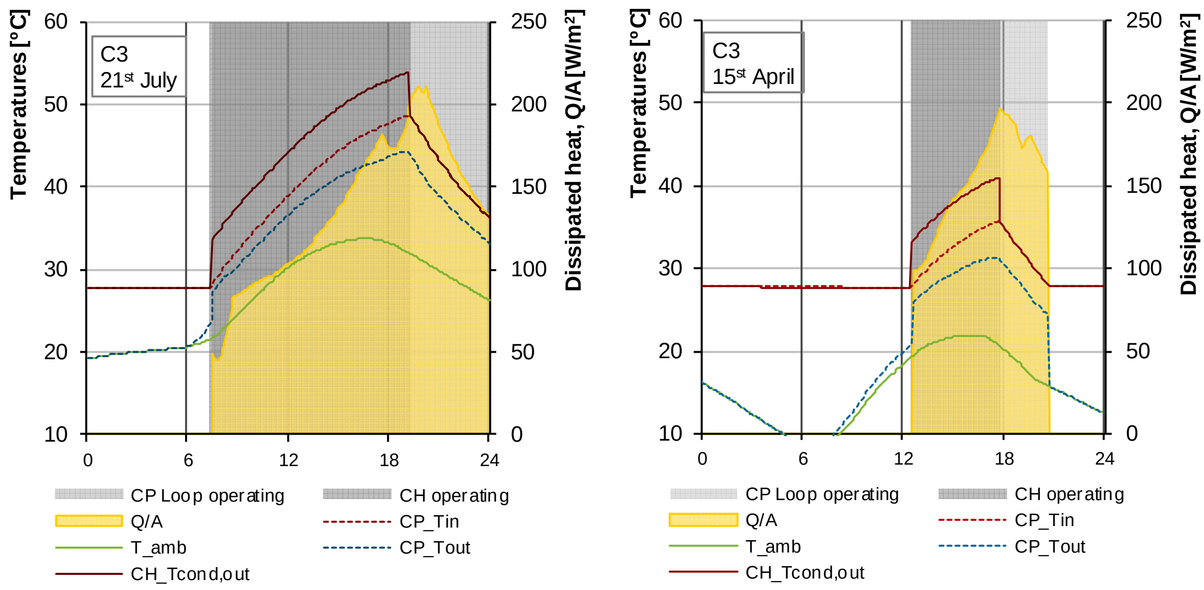

Figure 12. Cooling panels' performance during two days in Configuration 3.

The heat dissipation ratios of the cooling panels in configuration C3 are higher than in C2 due to the higher working temperatures. The increase of temperatures is due to the inability of the panels to maintain a constant temperature in the tank. The maximum condenser inlet temperature, recorded in the late afternoon, is 48.6ºC. Nevertheless, the working temperatures achieved are always within the working temperatures of the chiller defined by the manufacturer (from 30 up to 55ºC). The increase of temperatures causes an increase of heat dissipation ratios, these being enough to dissipate the heat rejected in the condenser.

The condenser inlet temperature defines the performance and consumption of the chiller, and the outlet temperature outlines the performance of the cooling panels loop. For this reason, two simulations have been carried out with configuration C1, with the two different condenser temperatures, in order to compare configuration $C1_{T30}$ with C2 and $C1_{T35}$ with C3 under the same working conditions.

3.2 Whole-system performance

To analyze the annual performance of the hybrid cooling system, the working hours of each loop and configuration are studied (Table 5) first. In $C1_{T30}$ and C2, where the inlet condenser temperatures are lower, the chiller working hours are shorter than those in $C1_{T35}$ and C3. This is due to the higher COP value of the first two options in comparison to the second two, where the performance is lower, so they require more working hours to achieve the set point temperature of the building.

Table 5. Hydraulic loops yearly working hours.

	Working hours			
	$C1_{T30}$	**C2**	**$C1_{T35}$**	**C3**
Building Tank Loop	3455	3256	3453	3262
Chiller Loop	1100	1100	1186	1182
CP Loop	0	1313	0	1898
CT	1100	930	1186	0

Configuration C2 includes the cooling panels in parallel to the cooling tower, in order to use the tower in the cases where the panels cannot maintain an outlet temperature of 30ºC. Considering a total of 1100 hours of chiller operation, cooling is provided exclusively with the cooling panels loop for only 130 hours. Thus, most of the time the cooling tower is needed to achieve the designed set point temperature of 30ºC. Even though in C3 the chiller works more hours, the system can reach the set point temperature of the building.

3.2.1 Energy consumption

The energy consumption considered in the analysis is the consumption of the chiller, on the one hand, and the consumption from the pumps and the cooling tower fan, on the other. In Figure 13 the annual total energy consumption of the four scenarios considered is shown, together with the mean inlet temperature of the condenser. The chiller consumption for configurations $C1_{T30}$ and C2 is similar, at 18.94 MWh. Configurations $C1_{T35}$ and C3 are also similar to each other, at 24.80 and 24.51 MWh respectively. This is due to the condenser inlet temperatures, which are the same for each pair. Yet, the pumps consumption increases as an additional pump is needed in C2 and C3 (P4).

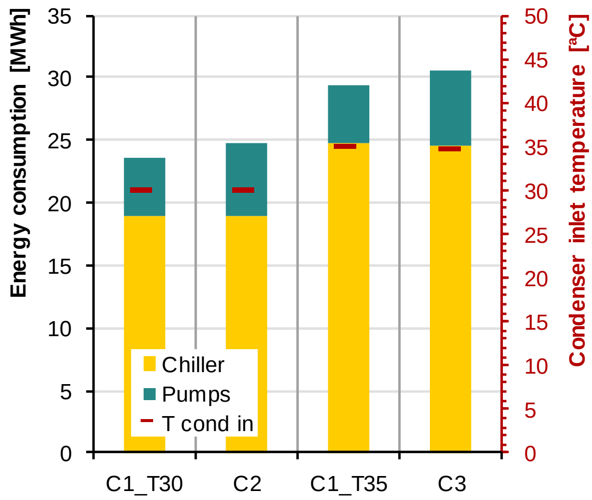

Figure 13. Yearly energy consumption (left axis) and average condenser inlet temperature (right axis).

The energy consumption in C2 is 4.7% higher than $C1_{T30}$ and C3 increases 3.6% compared to $C1_{T35}$. The pump with the highest consumption is the building loop pump (P1), since its operating hours are much higher. This consumption is maintained at every scenario. The consumption of the cooling tower fan is much lower than the pumps' consumption. When this element is eliminated, in C3, the savings obtained will be counteracted by the consumption of P4.

Regarding the heat rejection, a small time step was used to accomplish the energy balance of the heat rejected by the chiller and dissipated by the cooling tower or cooling panels. As shown in the graph (Figure 14), the heat rejected by the chiller is always the same as the heat rejected by the cooling towers or cooling panels.

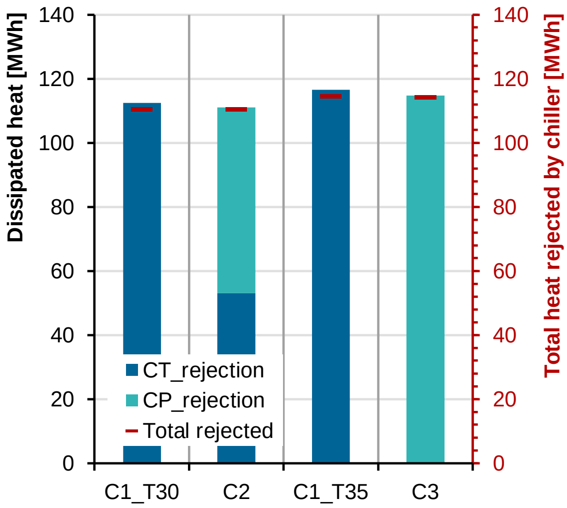

Figure 14. Heat rejection in the CT and CP loop.

In C2, the heat rejected by cooling panels is more than half of the total, which is in accordance with the working hours of each. All the heat rejected by the chiller is dissipated by cooling panels in C3.

3.2.2 Water consumption

The water consumption considered in this section is the water evaporated into the air stream and the blowdown water, estimated as explained in 2.4.2.

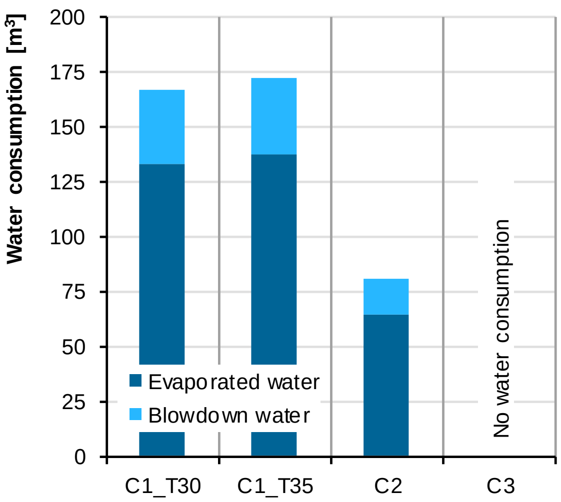

Figure 15. Yearly total makeup water of the cooling tower.

In C1 scenarios, the yearly consumption is 167 m^3 in the first case and 172 m^3 in the second (Figure 15). The water consumption decreases by half with the inclusion of cooling panels in C2, and logically, disappears completely in C3. The drift water is not considered as consumed water, yet it is the main risk source for legionella bacteria dispersion. In C3 the risk of legionella outbreak disappears since there is not cooling tower and consequently the drift water is non-existent.

3.2.3 Operation and maintenance cost estimation

The hybrid system presents advantages such as the elimination of water consumption and the environmental consequences that accompany this issue. In contrast, since cooling towers require little electricity to operate, the inclusion of radiant cooling panels leads to a small increase in electrical consumption compared to the conventional C1 systems, due to the additional pump needed by them.

However, the main annual cost of cooling towers is not the energy consumption but rather the maintenance cost. Most of the maintenance is related to water treatment control and legionella risk control. The cost of the maintenance of cooling towers varies considerably, depending on the size of the facility and country. In this case, two reference studies from Spain are considered to estimate the annual cost [39] [40]. Including the maintenance of the filling and cooling tower components, the legionella prevention tests, water treatment, the annual inspections by local authorities and an additional percentage in case of possible breakdowns, the total cost of the maintenance of a cooling tower may vary between 4,462 and 6,842 euro per year, not including labour, or about 5,500 €/year including labour. The maintenance of radiant cooling panels is minimal and is estimated at 500 € per year. The cost of the pumps' maintenance has not been included since it is the same for all scenarios. The maintenance cost of the additional pump needed for the cooling panels is included in the panel's maintenance estimate.

The electricity cost in Spain for non-residential customers is set at 0.13 €/kWh, incl. taxes [41]. Water is a local matter in Spain and its cost varies considerably depending on the city, so 1.89 €/m^3 is taken as an average value [42]. Bearing in mind the energy and water consumption presented in sections 3.2.1 and 3.2.2, and adding the maintenance cost, the annual operation and maintenance costs are summarized in Table 6.

Table 6. Estimates of yearly energy, water and maintenance costs of each configuration.

	Energy consumption [€/year]	Water cost [€/year]	Maintenance [€/year]	Total cost [€]
$C1_{T30}$	3068	315	5500	8883
$C1_{T35}$	3825	325	5500	9650
C2	3214	151	6000	9365
C3	3961	0.0	500	4461

The highest yearly operation and maintenance cost is that of $C1_{T35}$ followed by C2, which has duplicated systems (both cooling tower and panels). Even though C3 represents the highest electricity consumption, it has no water consumption and the maintenance cost is much lower than the systems that include cooling towers. Therefore, the annual total operation and maintenance cost of the hybrid system in C3 is estimated to be less than half of $C1_{T35}$, taking as a reference the simulated results.

3.2.4 *Comparison with current alternatives*

The existing alternative to cooling towers are water/glycol based, closed-loop air cooled systems [43], which do not consume water and therefore they do not present any legionella risk. However, they involve several downsides in comparison to cooling towers. Dry coolers are air condenser systems that reject heat forcing an air flow through a cooling coil. This equipment's cooling capacity limit is the dry bulb temperature instead of wet bulb temperature. Due to this limitation, air condensing systems are less efficient than water condensing ones. Besides, the fans needed for the forced convection cause a higher electrical consumption and noise. As with the cooling panels, given their dependency on the ambient temperature, the outlet temperature of dry coolers, i.e. $T_{cond,in}$, is more variable than that of the cooling towers.

In order to compare the cooling panels with the performance of dry coolers, a simulation has been run ($C1_{dry\ coolers}$) taking as a base $C1_{T35}$ scenario and replacing the cooling tower by a dry cooler (type 511). In this case, a 121.9 kW of nominal capacity dry cooler is chosen [43], with a design air flow rate of 15.75 kg/s and with four fans of 1.4 kW power each. Water is used as fluid.

In Table 7 the annual energy consumptions of the configurations presented in 3.2.1 are shown itemized, together with the results obtained in the $C1_{dry\ coolers}$ simulation. The table shows that the dependence of $T_{cond,in}$ of the different systems on the dry bulb temperature is more variable than those with cooling towers. The standard deviation rises up to 4.1ºC in the most variable case (C3).

Table 7. Yearly results of condenser temperature and energy consumptions of components.

	$T_{in,cond}$ [ºC]	Chiller	P1	P2	P3	P4	Fans	Total
	mean ± sd	**[MWh]**	**[MWh]**	**[MWh]**	**[MWh]**	**[MWh]**	**[MWh]**	**[MWh]**
$C1_{T30}$	30.1 ± 0.3	18.94	2.51	0.88	1.10	0.00	0.29	**23.61**
$C1_{T35}$	35.0 ± 0.3	24.80	2.41	0.95	1.19	0.00	0.08	**29.43**
C2	30.1 ± 0.7	18.94	2.39	0.88	1.10	1.31	0.10	**24.72**
C3	34.7 ± 4.1	24.51	2.41	0.95	0.71	1.90	0.00	**30.48**
$C1_{dry\ coolers}$	35.3 ± 3.3	25.10	2.41	0.94	1.17	0	4.18	**33.80**

When comparing the total energy consumption of the systems, The $C1_{dry\ coolers}$ configuration presents the highest energy consumption, followed by C3, though, these correspond to the only scenarios where the complications caused by water use are avoided. As expected, the fans of the dry cooler are the cause of increased electricity consumption. The dry cooler fan consumption is generally considered within the range of 10 and 20% of the total chiller and fans consumption [44]. In this case, the dry coolers consumption ratio is 14%. The total consumption of $C1_{dry\ coolers}$ is 10.9% higher than C3 and 14.8% higher than $C1_{T35}$.

4. Discussion

The analysis demonstrates that the hybrid cooling system is a feasible alternative to cooling towers, eliminating the drawbacks caused by such equipment, including the risk of legionella and water usage. It must be emphasized that given the environmental conditions and the case study building, the defined set point temperature was met in every configuration. The C2 scenario, where the cooling panels are installed in parallel to a cooling tower, served as a first approach to evaluate the performance of the cooling panels. In option C3, the cooling tower is replaced completely by the cooling panels. The mean heat dissipation ratio obtained in C2 is 104.9 W/m^2, while in C3 this value is increased to 147.0 W/m^2 given the higher working temperatures and therefore the higher temperature difference with the environment. The performance of the panels is not good enough to maintain the initial condenser inlet design temperature in C2, which is set at 30ºC. However, when the design working temperature of the condenser is increased to an average value of 35ºC, the cooling panels can dissipate the heat rejected by the chiller without the need of cooling towers (configuration C3). Two specific days of the year are analyzed, an average mid-day in April and the warmest day of the year, corresponding to 21st of July in Bilbao. In C3, the maximum inlet temperature of the condenser, at 48.6ºC simulated for the hottest day in July, is within the temperature range recommended by the manufacturer. Nevertheless, further research on the effect of high condenser temperatures on the lifespan of the chiller should be conducted.

Several parameters may limit the applicability of the system, and may represent opportunities for improvement:

- The shape of the building, the volume that needs to be cooled and the available façade surface can limit the use of panels. As Zhang and Niu say in [12], low-rise buildings are better suited to utilizing the nocturnal radiative cooling technology than high-rise buildings, because it is easier for the ratio of the radiator area to the building area to reach a desired value.
- Another field to be studied in depth is the application of cooling panels in low power chillers or heat pumps. As explained above, the higher the chiller power, the higher the fluid flow rate of the condenser. Thus, the building heat that the panels must absorb from the cooling fluid and then dissipate to the environment can be a limitation, depending on the available surface of cooling panels. Low power equipment may allow implementation of novel combinations of the external condenser component of the equipment. The increase of the fluid flow rate of the panels should also be experimentally tested.
- Due to their dependency on dry bulb temperature, cooling panels operate better at higher fluid temperatures, so facilities with high design temperatures would benefit more from such systems. However, this type of facility is focused on industrial applications, where the installed power is high, and so are the working fluid flow rates. Therefore, the useful surface might be a limitation to absorb the required flow rates.
- Recent advances made in radiative cooling under direct sunlight [20] [45] [46] have demonstrated the potential for achieving relatively high cooling output for a radiator at air temperature. However, as Erell and Etzion demonstrated, a building may be cooled only if the emitting surface is cooler than the indoor temperature [8]. This requires clever integration of the radiant cooling panels in a cooling system that is capable of transferring internal heat to the

emitting surface. The design of the panels should also solve their integration in the façade as an external layer, possibly employing them as shading devices to reduce heat gains through the envelope [47].

- A more constant temperature of the tank must be obtained towards an optimized system. It is known that the chiller capacity is sensitive to the variation of the fluid temperature exiting the cooling tower or cooling panels in this case [48]. Thus, both the cooling capacity of the panels and the tank design are key parameters to obtain a more constant temperature.
- A comprehensive cost analysis of the system should be made, including the manufacturing cost of the component, the initial investment in the cooling panel's installation and further design of their integration in the façade. In addition to this, the complete life cycle cost, covering both the running cost and the initial investment should be made.

The model of the hybrid system used in this simulation-based study has only been validated in a component scale, with the heat dissipation panel, therefore, to achieve greater reliability in the future, experiments of the complete hybrid system must be carried out to estimate the accuracy of the simulations.

5. Conclusions

This paper presents a performance assessment of a hybrid cooling system designed to be integrated in a building facade with the aim of replacing or complementing open circuit cooling towers. The hybrid system is presented as an alternative to highly selective surfaces for daytime radiative cooling recently developed, by using heat dissipation panels connected to the condenser of a conventional chiller. Thus, the working temperatures for the cooling panels are higher than in a passive cooling system and consequently the panels are able to dissipate heat during daytime. Two configurations of the hybrid cooling system (C2 and C3) were considered for the analysis evaluated through a comparative analysis with an existing 'conventional' system by simulation-based results.

In the scenarios studied, the use of the hybrid system requires between 3.6 and 4.7% *more* electrical energy on an annual basis. However, considering operation and maintenance, the C3 scenario presents the lowest total annual cost, about 50% *less* than comparable configurations with cooling towers. When comparing the hybrid system to an air heat dissipation system based on dry coolers, which is the current option available in the market, the results show that the annual energy consumption is 10.9% lower with the use of cooling panels. Thus, in terms of energy performance and in comparison to dry coolers, radiant cooling panels are a viable option.

The study demonstrates that an overall assessment of the advantages and disadvantages of a system must be made, and not just the electrical consumption, which is usually the main parameter considered when comparing design alternatives. Further studies about the optimization of the cooling panels and economic analysis of the initial investment of the façade must be made towards a future implementation of this solution in real buildings.

Nomenclature

α_s	solar absorptivity (-)
A	surface area (m^2)
a	solid surface area (m^2)
c_e	specific heat (kJ/kg·K)
C_s	thermal conductivity of the bond (W/m·K)
C_t	turbulent natural convection constant ($W/m^2K^{4/3}$)
d_t	distance between tubes (mm)
D	diameter (mm)
ρ	density (kg/m^3)
σ	Stefan-Boltzmann constant ($W/m^2 \cdot K^4$)
ε	emissivity (-)
F'	efficiency factor (-)
F_R	heat removal factor (-)
h	heat transfer coefficient ($W/m^2 \cdot K$)
I	solar radiation (W/m^2)
L	height (m)
$\dot{m}$	mass flow rate (kg/s)
q	volumetric flow rate (l/min)
$\dot{Q}$	total heat transfer (W)
$\dot{Q}/A$	total heat transfer per unit area (W/m^2)
R^2	coefficient of determination
$\dot{S}$	solar radiation on surface (W/m^2)
U	thermal transmittance (W/m^2K)
U_L	overall thermal losses coefficient ($W/m^2 \cdot K$)
T	temperature (°C)
v	wind velocity (m/s)

Subscripts

amb	ambient
cond	condenser
conv	convective
exp	experimental
ext	external
in	inlet
int	internal
mod	model
nat	natural
out	outlet
p	panel
rad	radiative
sp	setpoint
w	wind

Abbreviations

CTE	*Código Técnico de la Edificación* / Spanish Technical Building Code
COC	Cycles of Concentration
COP	Coefficient of Performance

CH	Chiller
CP	Cooling panels
CT	Cooling tower
DOE	Department of Energy of the United States
PV	Photovoltaic
RITE	*Reglamento de Instalaciones Térmicas en los Edificios* / Regulation of Thermal Installations in Buildings
TMY	Typical Meteorological Year

References

[1] IEA. The Future of Cooling: Opportunities for energy-efficient air conditioning Together Secure Sustainable. 2018.

[2] IEA. Energy Technology Perspectives. 2017.

[3] Santamouris M. Cooling the buildings – past, present and future. Energy and Buildings 2016;128:617–38. doi:10.1016/j.enbuild.2016.07.034.

[4] Day AR, Jones PG, Maidment GG. Forecasting future cooling demand in London. Energy and Buildings 2009;41:942–8. doi:10.1016/j.enbuild.2009.04.001.

[5] Santamouris M, Kolokotsa D. Passive cooling dissipation techniques for buildings and other structures: The state of the art. Energy and Buildings 2013;57:74–94. doi:10.1016/j.enbuild.2012.11.002.

[6] Santamouris M, Asimakopoulos DN. Passive cooling of buildings. James & James Science Publishers; 1996.

[7] Ito S, Miura N. Studies of Radiative Cooling Systems for Storing Thermal Energy. Journal of Solar Energy Engineering 1989;111:251. doi:10.1115/1.3268315.

[8] Erell E, Etzion Y. Radiative cooling of buildings with flat-plate solar collectors. Building and Environment 2000;35:297–305. doi:10.1016/S0360-1323(99)00019-0.

[9] Lu X, Xu P, Wang H, Yang T, Hou J. Cooling potential and applications prospects of passive radiative cooling in buildings: The current state-of-the-art. Renewable and Sustainable Energy Reviews 2016;65:1079–97. doi:10.1016/j.rser.2016.07.058.

[10] Bilbao JI, Sproul AB. Night Radiative Cooling with Unglazed PVT-Water Collectors: Experimental Results and Estimation of Cooling Potential. Proceedings of the ISES Solar World Congress 2015, Freiburg, Germany: International Solar Energy Society; 2016, p. 1–8. doi:10.18086/swc.2015.10.10.

[11] Tevar JAF, Castaño S, Marijuán AG, Heras MR, Pistono J. Modelling and experimental analysis of three radioconvective panels for night cooling 2015;107:37–48. doi:10.1016/j.enbuild.2015.07.027.

[12] Zhang S, Niu J. Cooling performance of nocturnal radiative cooling combined with microencapsulated phase change material (MPCM) slurry storage. Energy and Buildings 2012;54:122–30. doi:10.1016/j.enbuild.2012.07.041.

[13] Zhao B, Hu M, Ao X, Huang X, Ren X, Pei G. Conventional photovoltaic panel for nocturnal radiative cooling and preliminary performance analysis. Energy 2019:677–86. doi:10.1016/j.energy.2019.03.106.

[14] Zhao B, Hu M, Ao X, Chen N, Xuan Q, Su Y, et al. A novel strategy for a building-integrated diurnal photovoltaic and all-day radiative cooling system. Energy 2019;183:892–900. doi:10.1016/j.energy.2019.06.166.

[15] Erell E. Radiative cooling. In: Santamouris M, editor. Advances in Passive Cooling, London: James & James Science Publishers; 2007, p. 303.

[16] Erell E, Etzion Y. A radiative cooling system using water as a heat exchange medium. Architectural Science Review 1992;35:39–49. doi:10.1080/00038628.1992.9696712.

[17] Etzion Y, Erell E. Low-Cost Long-Wave Radiators for Passive Cooling of Buildings. Architectural Science Review 1999;42:79–85. doi:10.1080/00038628.1999.9696856.

[18] Mihalakakou G, Ferrante A, Lewis JO. The cooling potential of a metallic nocturnal radiator. Energy and Buildings 1998;28:251–6. doi:10.1016/S0378-7788(98)00006-1.

[19] Meir M, Rekstad J, Lovvik M. A study of a polymer-based radiative cooling system. Solar Energy 2002;73:403–17. doi:10.1016/S0038-092X(03)00019-7.

[20] Raman AP, Anoma MA, Zhu L, Rephaeli E, Fan S. Passive radiative cooling below ambient air temperature under direct sunlight. Nature 2014;515:540–4. doi:10.1038/nature13883.

[21] Aili A, Zhao D, Lu J, Zhai Y, Yin X, Tan G, et al. A kW-scale, 24-hour continuously operational, radiative sky cooling system: Experimental demonstration and predictive modeling. Energy Conversion and Management 2019;186:586–96. doi:10.1016/j.enconman.2019.03.006.

[22] ASHRAE. Cooling Towers. ASHRAE Handbook, 2012, p. 1–68.

[23] Zuazua-Ros A, Martín Gómez C, Ramos JC, Bermejo-Busto J. Towards cooling systems integration in buildings: Experimental analysis of a heat dissipation panel. Renewable and Sustainable Energy Reviews 2017;72:73–82. doi:10.1016/j.rser.2017.01.065.

[24] ASHRAE. Interaction with the local environment-ASHRAE Green Guide. Ashrae 2004:167–93.

[25] Marcó Gratacós J, Martí Costa S, Martín Zorraquino JV, Pastor Pérez P, Rodríguez Tarodo JA. Guía técnica para la prevención y control de la legionelosis en instalaciones - Technical guide for the prevention and control of legionellosis in building services. Madrid: 2006.

[26] Grosso M, Fracastoro, Vincenzo G, Simonetti M, Chiesa G. A hybrid passive cooling wall system: concept and laboratory testing results. Energy Procedia 2015;78:79–84. doi:10.1016/j.egypro.2015.11.118.

[27] Garay-Martinez R, Arregi-Goikolea B, Bonnamy P, Raji S, Lopez J. Concept, development and thermal characterization of an unglazed solar thermal collector for façade integration. Dyna (Spain) 2017;92:466–72. doi:10.6036/8108.

[28] Cui Y, Wang Y, Zhu L. Performance analysis on a building-integrated solar heating and cooling panel. Renewable Energy 2015;74:627–32. doi:10.1016/j.renene.2014.08.076.

[29] Zuazua-Ros A, Ramos JC, Martín-Gómez C, Gómez-Acebo T. Experimental assessment and model validation of a vertical cooling panel. Energy and Buildings 2017;142. doi:10.1016/j.enbuild.2017.02.062.

[30] Carrier Corporation. 30RW/30RWA Water cooled chillers.

[31] CTE. CTE - Documento Básico de Ahorro de Energía (DB - HE) 2019. https://www.codigotecnico.org/index.php/menu-ahorro-energia.html.

[32] University of Wisconsin-Madison. Solar Energy Laboratory. TRNSYS 17: Transient Simulation Program 1975.

[33] Eicker U, Dalibard A. Photovoltaic–thermal collectors for night radiative cooling of buildings. Solar Energy 2011;85:1322–35. doi:10.1016/j.solener.2011.03.015.

[34] Baker DR, Shryock HA. A Comprehensive Approach to the Analysis of Cooling Tower Performance. SPX Cooling Technologies, INC 2016:1–16. https://spxcooling.com/library/detail/a-comprehensive-approach-to-the-analysis-of-cooling-tower-performance.

[35] Kröger DG. Air-cooled heat exchangers and cooling towers. Penwell Corp; 2004.

[36] Walther E. California Statewide Utility Codes and Standards Program ASHRAE 90.1-related and Cooling Towers Topics Stakeholder Meeting #2. 2011.

[37] US DOE. Cooling Towers: Understanding key components of cooling towers and how to improve water efficiency 2011. https://www.energy.gov/sites/prod/files/2013/10/f3/waterfs_coolingtowers.pdf.

[38] Holmes JD. Wind loading of structures. Third Edit. CRC Press; 2017.

[39] Mor Fernández JM. Problemática sanitaria y ambiental de las torres de refrigeración y condensadores evaporativos.Estudio y control de la legionelosis en L'Hospitalet de Llobregat 2004.

[40] Cuadra Gamir J. Estudio económico de sustitución de torre de refrigeración evaporativa por equipo generados de frío. Málaga: 2015.

[41] Eurostat. Electricity prices for non-household consumers, first half 2018. Eurostat 2018. https://ec.europa.eu/eurostat/statistics-explained/index.php.

[42] Instituto Nacional de Estadística. España en cifras 2018. 2018.

[43] Carrier Corporation. 09FC Dry coolers /Air-cooled condensers.

[44] Rauser HC, Filippini S. Influence of the Dry Cooler Capacity on the Efficiency of Chillers. REHVA Journal 2015.

[45] Naghshine BB, Saboonchi A. Optimized thin film coatings for passive radiative cooling applications. Optics Communications 2018;410:416–23. doi:10.1016/J.OPTCOM.2017.10.047.

[46] Hossain MM, Gu M. Radiative cooling: Principles, progress, and potentials. Advanced Science 2016;3:1–10. doi:10.1002/advs.201500360.

[47] Etzion Y, Erell E. The thermal behavior of a concrete 'finned' wall in a hot-arid zone. Energy and Buildings 1991;17:331–5. doi:10.1016/0378-7788(91)90015-U.

[48] Wang L, Lee EWM, Yuen RKK. A practical approach to chiller plants' optimisation. Energy and Buildings 2018;169:332–43. doi:10.1016/J.ENBUILD.2018.03.076.

Highlights:

- Integration of cooling panels in a hybrid system is analyzed.
- The replacement of an open circuit cooling tower with cooling panels is achieved.
- The potential of the cooling panels is assessed.
- Hybrid cooling system established as alternative to cooling towers.
- Facade components integration with HVAC system is proposed.

Declaration of interests

☒ The authors declare that they have no known competing financial interests or personal relationships that could have appeared to influence the work reported in this paper.

☐The authors declare the following financial interests/personal relationships which may be considered as potential competing interests: